OPTIMAL CRUISE CONTROL OF HEAVY-HAUL TRAIN EQUIPPED WITH ELECTRONIC CONTROLLED PNEUMATIC BRAKE SYSTEMS

M. Chou, X. Xia

Department of Electrical, Electronic and Computer Engineering, University of Pretoria, Pretoria, 0002, South Africa

Abstract: In this paper a closed-loop cruise controller to minimise the running costs of the heavy-haul train is proposed. Consideration is given to velocity tracking, in-train force and fuel consumption, as well as optimisation of them. To overcome the communication constraints, a fencing concept is introduced whereby the controller is reconfigured adaptively to the current track topology. Simulation results on comparisons between different configurations are given: open-loop versus closed-loop; optimal velocity tracking versus optimal energy usage; and the improvement of adaptive fencing over general closed-loop control.

Keywords: train control, closed-loop, cruise control, LQR control method, optimal control, Electronic Controlled Pneumatic brake system(ECP).

1. INTRODUCTION

The main strength of South African's export lies in its mineral exports, rare metals such as platinum and gold as well as energy source such as coal. As most mines are situated inland, heavy-load transportation system is required to move the minerals to the harbours. Out of all the transportation means, railway proves to be the most economical.

The running cost of a train can be attributed to three main factors: energy consumption, travelling time and maintenance, mostly caused by in-train forces in the case of long trains.

In a scenario posed by Howlett (1996), an optimal control strategy for energy consumption for a diesel-powered passenger train was demonstrated. A similar method was also proposed by Khmelnitsky (2000). A subtle but important control problem is the slip control. The aim is to keep wheel slip around the point that produces the maximum friction coefficient for maximum adhesive force. Such studies include slip-detection system (Watanabe and Yamashita (2001)) to slip controller(Ishikawa and Kawamura (1997)). In-train force control and advanced high level controller, such cruise controller found in passenger trains, are missing for heavy-haul trains. One such controller is the H_2/H_∞ cruise control by Yang and Sun (2001).

In the current pneumatic controlled brake system (Garg and Dukkipati (1984)), signal propagation of the pressure wave used is limited to the speed of sound. As the train length typically exceeds 2.5km, this result in signal delay that causes uneven braking throughout the train. Another limitation is that individual brake is impossible since only one control signal is available.

The new electronic controlled pneumatic (ECP) brake system, discussed in Kull (2001), uses pneumatic brakes, but utilizes electronic control signals. Advantages are almost simultaneous brake control by wire and individual brake setting, which in theory, would be the most efficient.

In practice, ECP system needs to overcome two problems. First, true individual control is limited by computation and bandwidth constraints. Secondly, the current manual control does not take advantage of the additional control inputs, nor does it utilize the new distributed power (DP) system, which allows nonconsecutive locomotives groups to operate independently.

The lack of existing train controller has prompted this study. The result is a cruise control controller that provides flexibility in optimisation objectives. To tackle the problem of the bandwidth problem, the controller proposes the use adaptive wagon fencing, whereby cars with similar track environment receive the same control inputs, dramatically reducing the number of control signals used and thus bandwidth requirement.

Spoornet, South Africa's railway provider, is the first in the world to gradually rolled out ECP equipped heavy-haul trains. With the current system, locomotives operates in unison, *i.e.* no DP system, and wagons are ECP equipped, but without individual control. Such setup is used in this study to allow direct comparison between current operation and the proposed controller. A full DP/individual controlled ECP system is included in the results to show the full potential of the system, and for future implementation.

This paper is divided into three parts: section 2 describes the generic train model used in the setup, section 3 investigates the control methods and section 4 is the simulated results.

2. TRAIN DYNAMICS

Most existing literatures on heavy-haul train control consider the train as a single mass body (Howlett (1996)). With the new ECP train, this approach is no longer sufficient. For this study, each car is considered as an individual mass connected by elastic couplers. This allows individual states of the cars to be analysed, which is required for in-train force calculations. A simplified version of the model was used in the passenger train study of Yang and Sun (2001).

2.1 Coupler system

The cars are connected either via the knuckle-like couplers or solid draw bars, which connect to the draft gears of the cars.

The draft gear, together with the coupler or draw gear, forms the coupler system, shown in Fig. 1. The knuckle-like coupler slack results in dead band in the force displacement response, shown in Fig. 2.

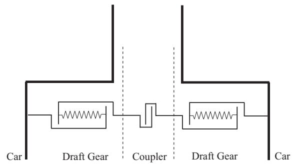

Fig. 1. Simplified schematic representation of the coupler system setup

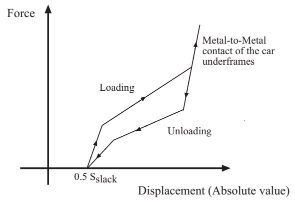

Fig. 2. Force displacement characteristic of the coupler system

To simplify the calculations of over hundreds of couplers found in a heavy-haul train, the coupler system is taken as a spring force,

$$F_{coupler} = k_i(x_i - x_{i+1}), \tag{1}$$

where spring constant k_i is the gradient of the curve in Fig. 2 and x_i and x_{i+1} are the displacements of the ith and $(i+1)$th wagons respectively.

This approximation holds well when draft gear travel is below the maximum. Once it reaches the maximum the coupler force becomes internal forces, which results in non-linear system. In this study, this non-linearity is approximated closely by using a linear system together with dynamic spring constants, which vary between the maximum and the normal value depending on the draft gear travel, and hard displacement limiters, which restraint the displacement within the limits.

2.2 Force model

The two major resistances experienced by a train are rolling resistance and aerodynamic drag, while the former is dominant at low speed operation. Aerodynamic drag is only considered for the first car, often the locomotive.

$$R = \underbrace{c_0 + c_v v}_{R^r} + \underbrace{c_a v^2}_{R^a}, \tag{2}$$

where v is the velocity of the car, R^r is the rolling resistance, R^a is the aerodynamic drag and the coefficients c_0, c_v, c_a are obtained experimentally.

In practice, certain train configurations couples four wagons via rigid bars into a group called a rake. These rakes are then connected via couplers. In our approach, these rakes are considered as a single entity with four times the mass and length of a wagon. The model is shown in Fig. 3.

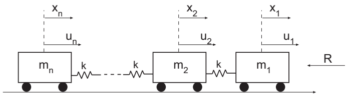

Fig. 3. Force diagram of the train.

In Fig. 3 n is the number of units, *i.e.*, rakes and locomotives. The equation of motion of the train is

$$\begin{aligned} m_1\ddot{x}_1 &= u_1 - k_1(x_1 - x_2) - (c_0 + c_v\dot{x}_1)m_1 \\ &\quad -c_a\dot{x}_1^2 M - 9.98\sin\theta_1 m_1 - 0.004D_1 m_1, \\ m_i\ddot{x}_i &= u_i - k_i(x_i - x_{i+1}) - k_{i-1}(x_i - x_{i-1}) \\ &\quad -(c_0 + c_v\dot{x}_i)m_i - 9.98\sin\theta_i m_i \\ &\quad -0.004D_i m_i, \quad i = 2, \ldots, n-1, \\ m_n\ddot{x}_n &= u_n - k_{n-1}(x_n - x_{n-1}) - (c_0 + c_v\dot{x}_n)m_n \\ &\quad -9.98\sin\theta_n m_n - 0.004D_n m_n, \end{aligned} \tag{3}$$

where $M = \sum_{i=1}^{n} m_i$, $\dot{x}_i$ and x_i are the velocity and the displacement of the car with respect to its own inertial frame; k_i is the spring constant; m_i and u_i are the mass and traction force of the ith unit respectively; $9.98m_i\sin(\theta_i)$ is the gravitational force with θ_i being the slope angle; curve resistance force is $0.004m_iD_i$, with curvature $D_i = 0.5d_{wheelbase}/R$ (Garg and Dukkipati (1984)) and R as the curve radius, as shown in Fig. 4.

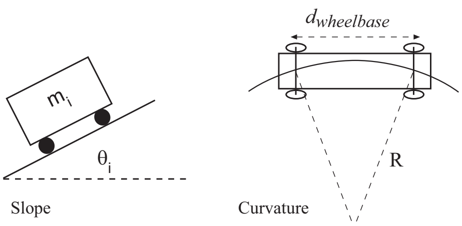

Fig. 4. Slope and curve angles.

Note that $u_i \leq 0$ if the ith unit is a rake. This is due to the fact that although the wagons are not powered in a heavy-haul train, they are still able to exert a braking force.

2.3 Parameters

The parameters used in the simulation are given in table 1. The values are based on the coal trains operating in South Africa by Spoornet.

Table 1. Heavy-haul train parameters.

Parameter	Value	Unit
No. of wagons	200	
No. of locos	6	
	Locomotive	
mass	103250	kg
c_0	7.6658×10^{-3}	Nkg^{-1}
c_v	1.08×10^{-4}	$Ns(mkg)^{-1}$
c_a	$2.06 \times 10{-}5$	$Ns^2(m^2kg)^{-1}$
k	$78 \sim 233 \times 10^6$	Nm^{-1}
Length	20.47	m
Max coupler slack	39.87×10^{-3}	m
Max traction	540	kN
Max brake	360	kN
	Wagon	
Loaded mass	104250	kg
c_0	6.3625×10^{-3}	Nkg^{-1}
c_v	1.08×10^{-4}	$Ns(mkg)^{-1}$
c_a	$1.4918 \times 10{-}5$	$Ns^2(m^2kg)^{-1}$
k	$29.29 \sim 49 \times 10^6$	Nm^{-1}
Length	12.07	m
Max coupler slack	77.5×10^{-3}	m
Max brake	100	kN
wheelbase dist.	8.310	m
	Track	
Slope θ	$-0.01 \sim 0.01$	rad
Min curve radius	300	m

3. CONTROLLER DESIGN

3.1 Open-loop controller

The open-loop controller calculates the forces required for the train to maintain the desired speed under current conditions. Using the force equation (3), the following results are obtained:

$$\begin{aligned} u_1 &= k_1(x_1 - x_2) + (c_0 + c_v v_d)m_1 + c_a v_d^2 M \\ &\quad + 9.98\sin\theta_1 m_1 + 0.004D_1 m_1, \\ u_i &= k_i(x_i - x_{i+1}) - k_{i-1}(x_{i-1} - x_i) \\ &\quad + (c_0 + c_v v_d)m_i + 9.98\sin\theta_i m_i \\ &\quad + 0.004D_i m_i, \quad i = 2, \ldots, n-1, \\ u_n &= -k_{n-1}(x_{n-1} - x_n) + (c_0 + c_v v_d)m_n \\ &\quad + 9.98\sin\theta_n m_n + 0.004D_n m_n, \end{aligned} \tag{4}$$

where v_d is the desired velocity.

The equations are under-determined in terms of variables $u_1, \ldots, u_n, x_1, \ldots, x_n$. Summing the equilibrium forces in equation (4), the total effective force required is

$$\begin{aligned} u_T &= u_1 + u_2 + \cdots + u_n \\ &\quad + \sum_{i=1}^{n} m_i(c_a v_d^2 + c_0 + c_v v_d + 9.98\sin\theta_i + 0.004D_i). \end{aligned} \tag{5}$$

There are no unique ways of distributing the forces $u_1, \ldots, u_n$ to satisfy equation (5). In this paper, we assume in open-loop control, the braking forces are all set to zero, and the required effective force u_T is equally distributed to the locomotives.

Once $u_1, \ldots, u_n$ are chosen according to equation (5), equation (4) can be used to uniquely determine $k_1(x_1 - x_2), \ldots, k_{n-1}(x_{n-1} - x_n)$. If we take the position of the leading car (usually a locomotive) x_1 as a reference, then in steady state, the relative positions (therefore, the in-train forces) are uniquely determined. These values are dependent on the traction forces of the locomotives, the braking forces of the wagons and the operation travelling speed.

3.2 Transient control

During velocity reference changes the open-loop control in (5) still exhibits steady-state errors due to factors such as modelling errors and parameter inaccuracy. To decrease this error, a planned acceleration term can be added to (5). The improved open-loop control force is then

$$U = Ma_d + u_T, \tag{6}$$

where a_d is the planned acceleration, which only last during an acceleration period t_a, determined by

$$t_a = \frac{v_d(i+1) - v_d(i)}{a_d}, \tag{7}$$

where $v_d(i+1)$ and v_d are the new and current reference speed respectively.

3.3 Closed-loop controller

From the model described by the force equation (3), following the linearization method described in Goodwin *et al.* (2001), the following state-space model can be found.

$$\dot{\boldsymbol{x}} = \begin{bmatrix} \mathbf{0}_{n\times n} & \mathbf{I}_{n\times n} \\ \mathbf{A}_{21} & \mathbf{A}_{22} \end{bmatrix} \boldsymbol{x} + \begin{bmatrix} \mathbf{0}_{n\times n} \\ \mathbf{B}_{21} \end{bmatrix} \boldsymbol{u}, \tag{8}$$

where

$$\mathbf{B}_{21} = \mathbf{I}_{n\times n}, \tag{9}$$

$$\mathbf{A}_{21} = \begin{bmatrix} -\frac{k_1}{m_1} & \frac{k_1}{m_1} & 0 & \ldots & 0 & 0 & 0 \\ \frac{k_1}{m_2} & -\frac{k_1+k_2}{m_2} & \frac{k_2}{m_2} & \ldots & 0 & 0 & 0 \\ \vdots & \vdots & \vdots & \ddots & \vdots & \vdots & \vdots \\ 0 & 0 & 0 & \ldots & \frac{k_{n-2}}{m_{n-1}} & -\frac{k_{n-2}+k_{n-1}}{m_{n-1}} & \frac{k_{n-1}}{m_{n-1}} \\ 0 & 0 & 0 & \ldots & 0 & \frac{k_{n-1}}{m_n} & \frac{-k_{n-1}}{m_n} \end{bmatrix}, \tag{10}$$

$$\mathbf{A}_{22} = \begin{bmatrix} -c_v - \frac{2c_a v_0 M}{m_1} & 0 & \ldots & 0 \\ 0 & -c_v & \ldots & 0 \\ \ldots & \ldots & \ldots & \ldots \\ 0 & \ldots & \ldots & -c_v \end{bmatrix}. \tag{11}$$

The state variables $\boldsymbol{x} = [\delta x_1 \ \ldots \ \delta x_n \quad \delta \dot{x}_1 \ \ldots \ \delta \dot{x}_n]$ and $\boldsymbol{u} = [\delta u_1 \ \ldots \ \delta u_n]$ are the deviations from the equilibrium point.

3.4 Fencing

In equation (9) ideal individual control is assumed. However, availability of control signal bandwidth prohibits this.

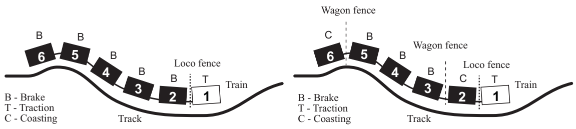

Fig. 5. Comparison between with and without adaptive fencing.

In the left of Fig. 5, car 6, although climbing uphill, has to apply its brake since the train only has one control signal for all the wagons. With adaptive wagon fencing, showing on the right of Fig. 5, wagon with similar track conditions are grouped and controlled together. The term fence refers to the separation of control signals.

The adaptive wagon fencing controller automatically calculates new fences for the train as it travels down the track.

$$F = [f_1, f_2, \ldots, f_j], \tag{12}$$

where f_j is the first car after the fence. The number of fences j and $\mathbf{B_{21}}$ will vary with the complexity of the track modulation.

$$\mathbf{B_{21}} = \begin{bmatrix} \mathbf{1}_{f_1-1} & \mathbf{0}_{f_1-1} & \ldots & \mathbf{0}_{f_{j-2}-1} & \mathbf{0}_{f_j-1} \\ & \mathbf{1}_{f_2-f_1} & \ldots & & \\ & & \ldots & \mathbf{1}_{f_{j-1}-f_{j-2}} & \\ \mathbf{0}_{n-f_1+1} & \mathbf{0}_{n-f_2+1} & \ldots & \mathbf{0}_{n-f_{j-1}} & \mathbf{1}_{n-f_j+1} \end{bmatrix}, \tag{13}$$

where $\mathbf{0}$ and $\mathbf{1}$ denote column vectors of 0 and 1 respectively.

The concept of adaptive fencing is well related to recent interests in the control community of reconfigurable/switching control systems (Wu (1995)).

To evaluate whether a new set of fences is required, the controller calculates the median of the slope angles and the track curvature the train experiences at each sampling time t_s. If either exceeds the previous value by a predefined threshold f_{th}, a new set of fences will be calculated.

From the leading car, the controller will add a fence between the current and the next unit under the following conditions:

(i) The unit type differs, *e.g.*, rake following a locomotive
(ii) The slope experienced by the next unit exceed the slope experienced by the previous fenced unit by a predefined threshold f_{seg}.
(iii) The above condition occurs for the track curvature.

3.5 LQR control

Based on the LQR optimisation method described in Goodwin *et al.* (2001), the cost function is defined as

$$J = \int \mathbf{x}'\mathbf{Q}\mathbf{x} + \mathbf{u}'\mathbf{R}\mathbf{u}, \qquad (14)$$

where $\mathbf{Q}$ and $\mathbf{R}$ are the weights.

To use LQR method, the running costs: in-train force, fuel consumption and travelling time need to be quantified. Fuel consumption is directly related to u. Thus the diagonal of the gain matrix R will determine the fuel consumption as well as brake usage, *i.e.*,

$$\mathbf{R} = \begin{bmatrix} r_1 & 0 & \dots & 0 \\ 0 & r_2 & \dots & 0 \\ \dots & \dots & \ddots & \dots \\ 0 & 0 & \dots & r_n \end{bmatrix}, \qquad (15)$$

where $r_i, i = i \dots n$ are the weighting coefficients for the traction and brake force on each car. When adaptive fencing occurs, the size n will change accordingly.

The weighting matrix Q is chosen such that

$$\mathbf{x}'\mathbf{Q}\mathbf{x} = q_0 x_1^2 + \sum_{i=1}^{n-1} q_{1i} k_i^2 (x_i - x_{i+1})^2 + \sum_{i=1}^{n} q_{2i} (\dot{x}_i - v_d)^2, \qquad (16)$$

in which all the q's are positive. The first term q_0 is chosen to penalise the travelling of the leading car and to satisfy an observability requirement (Goodwin *et al.* (2001)) for solving the LQR problem. The second term is to penalise the in-train forces experienced by the couplers, and the third term is to penalise the travelling speed tracking of the whole train.

Although the closed-loop controller will not be able to optimise the travelling time and fuel efficiency at the global level, through cost coefficients q_{2i} and r_i travelling time and fuel consumption can be optimised locally, *i.e.*, at the current track position.

4. RESULTS

The simulated train setup utilises the parameters specified in table 1 with a sampling time $t_s = 10ms$. The locomotives are split into two groups, four in the front and two in the rear. The train has an initial velocity of $10ms^{-1}$. The reference velocity changes to $15ms^{-1}$ at the $5.5km$ point and $8ms^{-1}$ after the $13km$ point.

In terms of the LQR controller, q_0 is chosen as 0.17 for all the simulations. The individual weights q_{1i} and q_{2i} are set equally. All weights r_i are chosen as 1. Weights $\mathbf{R}$ and q_{2i}'s are multiplied by the maximum of the k_i set to bring them around the same magnitude as weight q_{1i}.

4.1 Open-loop versus closed-loop

Looking at closed-loop control in Fig. 7, with weight values $q_{1i} = 1$, $q_{2i} = 1$, it is clear that velocity tracking has improved tremendously over open-loop (Fig. 6). However, in-train force levels are higher. By reducing q_{2i}, one can trade off velocity tracking with better in-train force, as shown in 8. All three setups utilize the single traction, single brake signal setup throughout the train.

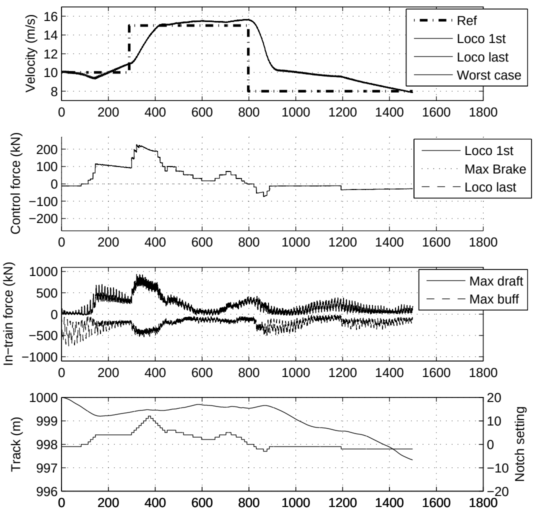

Fig. 6. Open-loop controller.

4.2 Fence control

Fig. 9 shows a setup with DP and individual ECP brake control to demonstrate the full potential of the system. Fencing is also applied to keep brake control signals used around a practical amount. The threshold values f_{th} and f_{seg} of 5×10^{-3} were used for slope angle, and 1×10^{-2} for curvature.

5. CONCLUSION

This paper presents a summary of a new heavy-haul train controller for the new ECP train. The controller is adaptive for different optimisation objectives: energy consumption, velocity tracking and in-train force. When implemented, this would allow drivers to change the optimisation objectives with respond to the current track condition.

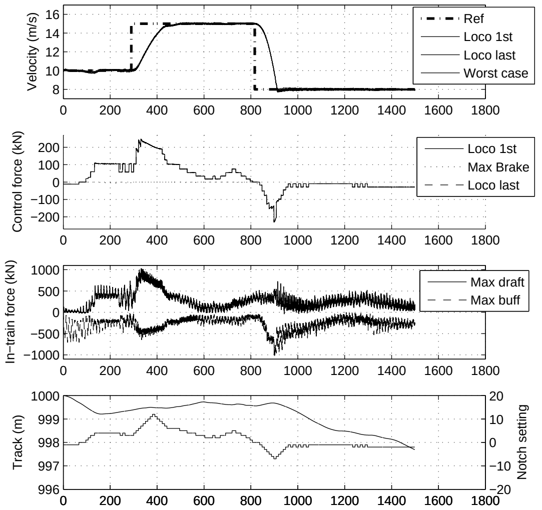

Fig. 7. Closed-loop controller (Optimised for velocity tracking).

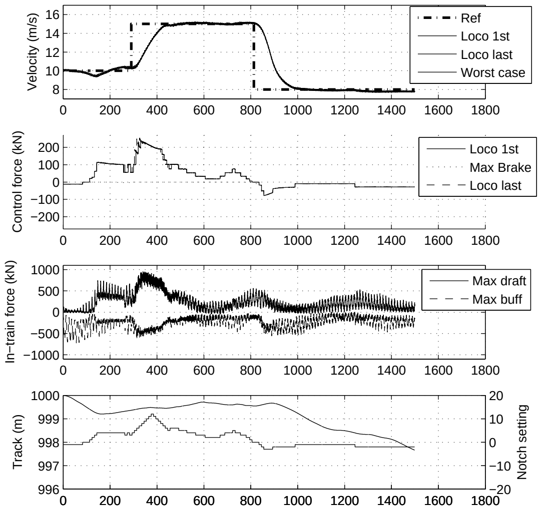

Fig. 8. Closed-loop controller (Optimised for in-train force).

For example velocity tracking could outweigh energy consumption when a train is late for shipment.

Notes that the closed-loop controller is able to show significant improvement even with the current limited train setup of only single traction signal and single ECP brake signal. The adaptive fence control achieves the advantages of individual wagon control while overcoming implementation constraints.

It can be stated that the new cruise controller has achieved its goal. With further testings and tuning, the implementation of such controller can be seen in the foreseeable future, minimising the

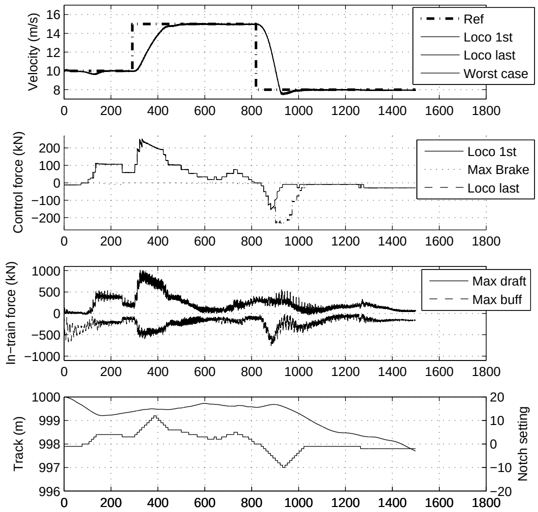

Fig. 9. Closed-loop controller, DP/full ECP train with fencing.

fourth running cost of heavy-haul train: human workload.

REFERENCES

Garg, V.K. and R.V. Dukkipati (1984). *Dynamics of Railway Vehicle Systems*. xiii ed.. Toronto: Academic Press.

Goodwin, G.C., S.F. Graebe and M.E. Salgado (2001). *Control System Design*. New Jersey: Prentice Hall.

Howlett, P. (1996). Optimal strategies for the control of a train. *Automatica* **32**(4), 519–532.

Ishikawa, Y. and A. Kawamura (1997). Maximum adhesive force control in super high speed train. *Proceedings of the Power Conversion Conference - Nagaoka* **2**, 951–954.

Khmelnitsky, E. (2000). On an optimal control problem of train operation. *IEEE Transaction of Automatic Control* **45**(7), 1257–1266.

Kull, R.C. (2001). Wabtec ecp system update. *Proceedings of the 2001 IEEE/ASME Joint Railroad Conference* pp. 129–134.

Watanabe, T. and M. Yamashita (2001). A novel anti-slip control without speed sensor for electric railway vehicles. *The 27th Annual Conference of the IEEE Industrial Electronics Society* **2**, 1382–1387.

Wu, N. (1995). Control design for reconfigurablility. *Proceedings of the American Control Conference* pp. 102–106.

Yang, C.D. and Y.P. Sun (2001). Mixed H_2/H_∞ cruise controller design for high speed train. *International Journal of Control* **74**(9), 905–920.